Journal of Petroleum Research and Studies

Open Access
Vol. 14, No. 3, September 2024, pp. 135-154

P- ISSN: 2220-5381
E- ISSN: 2710-1096

DOI: http://doi.org/10.52716/jprs.v14i3.865

Investigation the Performance of an Evacuated Tube Solar Collector Filled with MWCNT/ Water Nanofluid Under the Climate Conditions of Al-Hilla (Iraq)

Nagham Yass Khudair[1*], and Ahmed Kadhim Hussein[2]

[1]Metallurgy Department, University of Babylon/ College of Materials Engineering, Babylon City. Hilla -Iraq.

[2]Mechanical Engineering Department, University of Babylon/ College of Engineering, Babylon City. Hilla -Iraq

[*]Corresponding Author E-mail: mat.nagham.yass@uobabylon.edu.iq

Received 24/12/2023, Revised 6/03/2024, Accepted 10/03/2023, Published 22/09/2024

Abstract

The main obstacles to securing the future of humanity are the rising energy demand and the constrained supply of conventional energy sources. In order to guarantee the sustainability of energy in this world for the present and the future, solar energy is a desirable source of energy. Solar thermal collectors with evacuated tubes are primarily employed in domestic settings. Even in low-temperature applications, replacing the working fluid with nanofluid can improve heat transfer. The effect of Multi-Walled Carbon Nanotubes (MWCNT) and water nanofluid as working fluids in evacuated tube solar collectors(ETSC) is used to investigate the collector's thermal performance experimentally. Three different volume fraction of (MWCNT) nanoparticles of (0.01%, 0.03% and 0.05%) were examined at various volume flow rates ranging from (1 to 3 L/min). Experiments were performed in Al –Hilla, Iraq. The results show an enhancement in the efficiency with increase in the volume fraction of(MWCNT)nanoparticles and volume flow rate (i.e. concentration (0.05%) and volume flow rate (3L/min). The temperature difference of the fluid at concentration (0.05%) and volume flow rate (1L/min) increased up to (86.84 %) with adding (MWCNT) nanoparticles compared with the water. The results showed, maximum efficiency enhancement of the collector at concentration (0.05%) and volume flow rate (3L/min) about (69.63%) compared with water.

Keywords: Solar energy, Multi-walled carbon nanotube (MWCNT), Evacuated Solar Collector Tube, Thermal Performance.

Journal of Petroleum Research and Studies

Open Access
Vol. 14, No. 3, September 2024, pp. 135-154

P- ISSN: 2220-5381
E- ISSN: 2710-1096

تقصي أداء المجمع الشمسي ذو الأنبوب المفرغ المملوء بمائع نانوي من انابيب الكاربون النانوية ذات الجدران المتعددة والماء تحت ظروف الحلة المناخية

الخلاصة:

أن التحدي الرئيسي الذي يواجه مستقبل البشرية هو زيادة الطلب على الطاقة ومحددات تجهيز مصادر الطاقة التقليدية. لغرض ضمان ديمومة الطاقة في هذا العالم ألان ومستقبلا فأن الطاقة الشمسية هي المصدر المرغوب من الطاقة. المجمعات الشمسية ذات الأنابيب المفرغة تستخدم بالأساس للأغراض المنزلية وايضاً في التطبيقات ذات الدرجات الحرارية المنخفضة حيث ان استبدال مائع التشغيل بالمائع النانوي يحسن انتقال الحرارة. ان تأثير استخدام المائع النانوي المتكون من أنابيب الكاربون النانوية ذات الجدران المتعددة والماء في المجمعات الشمسية ذات الأنابيب المفرغة قد تم دراسته تجريبيا. ثلاث كسور حجميه مختلفه من جسيمات أنابيب الكاربون النانوية ذات الجدران المتعددة وهي (0.05, 0.03, 0.01)% تم اختيارها تحت معدل تدفقات حجميه مختلفة (1-3 L/min) تجارب اجريت في الحلة – العراق. أوضحت النتائج زيادة في الكفاءة مع زيادة الكسر الحجمي لجسيمات أنابيب الكاربون النانوية ذات الجدران المتعددة ومعدل التدفق الحجمي أي عند تركيز (0.05%) و (3 L/min) ان فرق الحراره للمائع عند تركيز (0.05%) ومعدل تدفق حجمي (1L/min) يزداد الى (86.84 %) مع اضافة جسيمات (MWCNT) مقارنة مع الماء. أوضحت النتائج ان اقصى تحسين في الكفاءة للمجمع عند تركيز (0.05%) ومعدل تدفق حجمي (3L/min) بحدود (69.63%) مقارنة مع الماء.

1. Introduction:

Solar energy can be replenished indefinitely and does not contribute to environmental pollution, it is increasingly being put to use in a variety of fields, including the production of electrical power, energy heating systems, and the processing of chemical substances. The Evacuated Tube Solar Collectors (ETSC) have the ability to collect the available Solar Energy and then transmit it to the water heating system in the form of thermal Energy [1–3]. The ETSCs are constructed out of a number of rows or parallel arrays of glass tubes. Each tube contains a coated twin glass tube that is capable of absorbing solar energy and is incorporated into the design. It is necessary to remove the air from the gap between the two glasses in order to create a vacuum. As a result, there is no air present to create convective losses or to transport heat, and therefore, both convective and conductive heat losses are eliminated. In the research that has been done on vacuum solar collectors, researchers have identified two primary categories: all-glass direct flow collectors and heat pipe ETSC collectors [4–6].

Using nanofluid to reach greater temperatures and increase efficiency is one of the recent alluring improvements in solar working fluids. Researchers have proposed using a variety of nanomaterials, including carbon nanotubes (CNT), copper oxides (CuO), aluminum oxides (Al_2O_3), and others, at various quantities and in various methods when it comes to using nanofluids in ETSC. Through a series of studies. [7]

Fully investigated the impact of CeO2/water nanofluid on the effectiveness of ETSC with a concentration of 0.035% and mass flux rate of 0.017 kg/s.m^2. They noticed that, the temperature

Open Access
Vol. 14, No. 3, September 2024, pp. 135-154
P- ISSN: 2220-5381
E- ISSN: 2710-1096

difference, heat removable factor and useful heat gain were increased by increasing volume concentration and mass flux rates. Also, they concluded that, the maximum increase in temperature difference, heat removable factor, heat gain was respectively (37.3%, 34.66% and 42.3%) at (φ=0.035% and $\dot{m}$=0.017 kg/s.m^2) compared with the pure water. [8], investigated experimentally the efficiency of (UTSC) by using (Al_2O_3 /water) nanofluid at different concentration, mass flow rate and nanoparticles size. It was found that, the thermal conductivity of (Al_2O_3) increased by increasing concentration of nanoparticles. Also, they concluded that the efficiency of (UTSC) increased by increasing mass flow rates and decreasing nanoparticles size. It was attained its maximum value (i.e.,72.4%) at highest mass flow rate and concentration equals to (1.0 vol.%). [9], investigated experimentally the thermal efficiency of (ETSC) by using (Cu/water) nanofluid at different volume concentrations and volume flow rates. The mean diameter of (Cu) nanoparticle was considered as (50nm). It was found that, the thermal efficiency of (ETSC) was increased by increasing volume concentrations and volume flow rates. Also, they concluded that absorbed and the removal energy parameters attained respectively their maximum values (i.e., 0.83 and 21.66) at highest value of volume concentrations of the nanofluid. [10]

Investigated experimentally the energy and exergy efficiencies of (ETSC) by using (MWCNT/ water) nanofluid at different weight fractions and volumetric flow rates. They used an artificial sunlight system to simulate the solar radiation in the laboratory of British University in Egypt. It was found that, both of the energy and energy efficiencies in (ETSC) were increased by increasing weight fraction and flow rates. Also they concluded that energy and energy efficiencies attained respectively their maximum values (i.e., 55% and 10%) at highest value of weight fraction of the nanofluid. As a result, in-depth experimental work was carried out to investigate the impact that incorporating MWCNT/water would have on the thermal performance of an evacuated tube collector.

We are confident that this work will contribute to an increase in the utilization of nanofluid in solar energy applications, which typically results in lower levels of carbon dioxide emission. In addition to this, it offers a profound insight into the use of MWCNT/water as a fluid with favorable thermal properties. In addition, the thermal performance of the nanofluids in the evacuated tube solar collector is evaluated for different operating temperatures, nanoparticle volumetric fractions, and mass flow rates. The main purpose of the present study is to investigate

Open Access
Vol. 14, No. 3, September 2024, pp. 135-154
P- ISSN: 2220-5381
E- ISSN: 2710-1096

the thermal performance enhancement of evacuated tube solar collector by using MWCNT nanofluids with different concentration of 0.01,0.03%and 0.05 %.

2. Methodology

2.1 Nanofluid preparation method

In accordance with the literature review, a single step method can be used to generate metal nanofluids, whereas a two-step method is preferable to prepare nanofluids containing oxide nanoparticles [11-16]. Nanofluid stabilization and low agglomeration are the two main issues with two-step techniques [17-20]. To prepare an even stable suspension, a number of procedures and approaches are used, such as the use of ultrasonic equipment, the addition of stabilisers, or pH control. The two-step approach will be used in this study to create (MWCNT/deionized water) nanofluids. Nanoparticles of (MWCNT) were purchased from Cheap Tubes, Inc., a firm situated in the United States of America. An improvement was made to ETSC by using nanofluids (MWCNT/DI) instead of regular fluid water. These nanofluids had three volume concentrations of nanoparticles made of (MWCNT) powders (0.01% ,0.03% and 0.05%) with purity≥ 99 percent, and they were mixed with deionized water together. Triton X-100, which is a natural surfactant, was utilized in this investigation as a base fluid. Additionally, water that had been deionized was employed for the purpose of dispersing MWCNT. Methods involving two steps were carried out in order to permit a reduction in the amount of aggregation caused by MWCNT and an increase in the scattering behavior. First, by utilizing Triton X-100 as a surfactant The three concentrations were mixed with deionized water for 1 hour using a magnetic stirrer and then sonicated for 4 hours. The sonicator had a frequency of 24 kHz and an amplitude of 60% with 0.5 s pulses. the following standard mathematical expressions are used to calculate the weights (particular volume concentration) of MWCNT nanoparticles.

$$\varphi = \frac{V_{np}}{V_{nf}} \quad (1)$$

$$V_{nf} = V_{np} + V_{bf} \quad (2)$$

$$V_{bf} = \frac{W_{bf}}{\rho_{bf}} \quad (3)$$

$$V_{np} = \frac{W_{np}}{\rho_{np}} \quad (4)$$

3. Experimental work

The objective of this study is to explore the efficiencies of a heat pipe evacuated tube solar collector that uses deionized water as its working fluid and operates at a variety of flow rates

Open Access
Vol. 14, No. 3, September 2024, pp. 135-154
P- ISSN: 2220-5381
E- ISSN: 2710-1096

ranging from one to three and a half liter per minute. The aperture area of the testing system was 1.128 m^2, and it was a commercial evacuated tube solar collector (ETSC). To achieve the greatest possible surface area for heat absorption, each heat pipe is positioned in the pipe's center and supported by an aluminum fin. The ETSC configuration that was used to perform the current experiments was installed in Hilla city (32° North 44° East), which is depicted in Figure (1 A and B), while Figure (2) illustrates a schematic diagram of the system. The characteristics of the collector are listed in Table (1). The tank has a capacity of one hundred and fifty liters (L), and it is linked to the collector by a coil heat exchanger, so completing the circuit for the working fluid. The connection between the collection and the tank is made using insulated CPVC tubing, which stands for chlorinated polyvinyl chloride. In the event that it was essential, control (on/off) valves were installed both before and after the collector in order to manage the flow of the fluid throughout the system. The instrumentations are as follows: four thermocouple sensors of type K, each of which is connected to a readout; the accuracy of the sensors is (0.4 degrees Celsius); the reading range is (-40 degrees Celsius to 150 degrees Celsius); and the reading range is as follows: Thermocouples are utilized for both the collector and the tank in order to measure the temperatures that can be found at the beginning and end of both the collection and the tank respectively. For the purpose of determining the rate at which the fluid was moving, a flow meter was utilized. Between the hours of nine in the morning and four in the afternoon, the ETSC was run by turning on the pump in order to get deionized water circulating through the system.

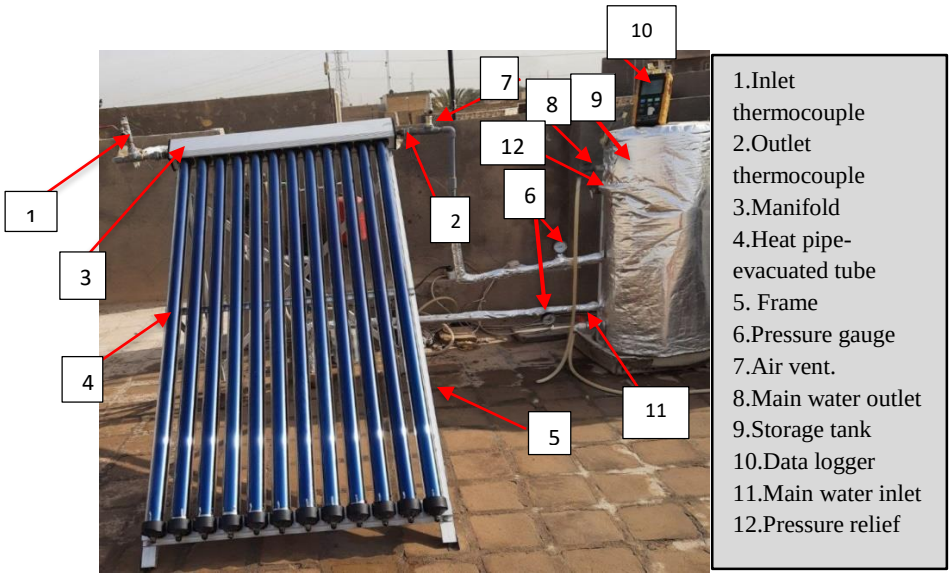

Fig. (1): (A) Photograph of evacuated tube solar collector used in the present work.

Journal of Petroleum Research and Studies

Open Access
Vol. 14, No. 3, September 2024, pp. 135-154

P- ISSN: 2220-5381
E- ISSN: 2710-1096

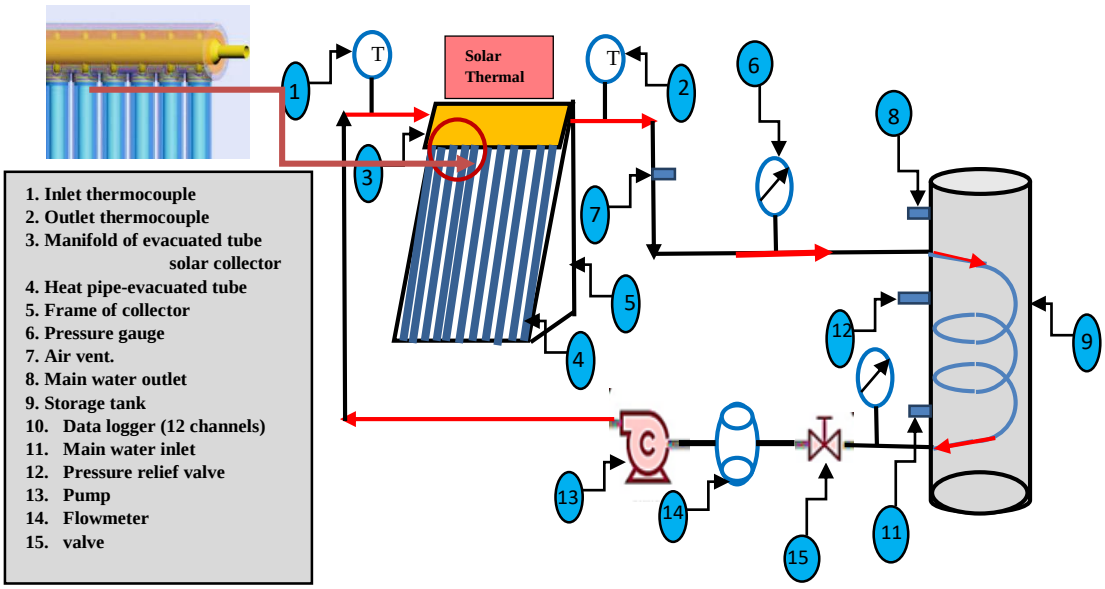

Fig. (1): (B) Solar Heating Unit Block

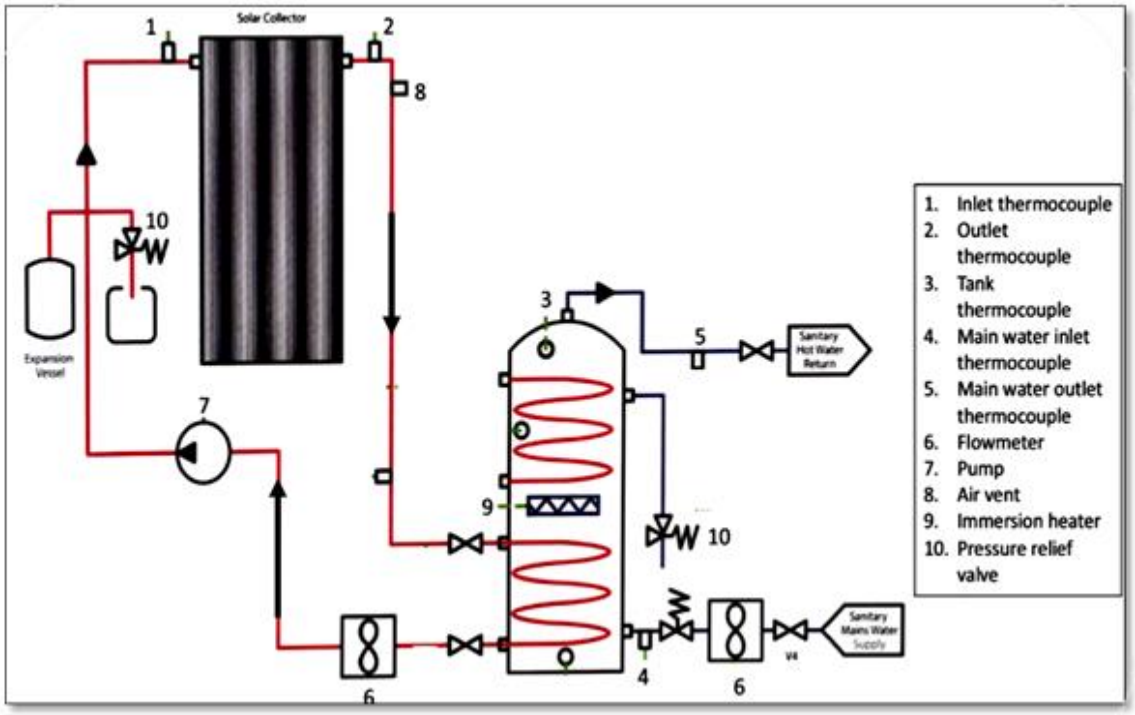

Fig. (2): Sensors locations in evacuated tube solar collector

Open Access
Vol. 14, No. 3, September 2024, pp. 135-154
P- ISSN: 2220-5381
E- ISSN: 2710-1096

Table (1) Heat pipe evacuated tube solar collector specification

Specification	Dimension
Active Area	1.128 m^2
Glass Transmissivity	$\tau \geq 92\%$
Absorber Emissivity	$\varepsilon \leq 8\%$
Absorber Coating Emissivity	$\varepsilon \leq 5\%$
Absorber Absorptivity	$\alpha \geq 92\%$
No. of Evacuated Tubes	12
Heat Pipe	Material: High purity copper Thermal conductivity: 401 W/m.k Inner diameter: 12mm Outer diameter: 14mm Fluid: Ethanol
Tube Length	180 cm
Outer Glass Tube	58 mm diameter Transmissivity $\tau \geq 92\%$ Emissivity $\varepsilon \leq 90\%$ Thickness 2 mm
Inner Glass Tube	47 mm diameter Outward Emissivity $\varepsilon \leq 35\%$ Inward Emissivity $\varepsilon \leq 8\%$ Thickness 2 mm
Manifold Insulation Thermal Conductivity	Ki = 0.043 W/m. K

4. Computations

The use of energy balance equations serves as the foundation for the thermodynamic modeling of an ETSC's energy system. Kalogirou and colleagues [21] compiled the equations for an ETSC in steady state for the purpose of calculating energy.

4.1 Energy efficiency

The balance equation of energy is given by:

$$\dot{Q}_u = \dot{Q}_{Abs} - \dot{Q}_{loss} \quad (5)$$

$$\dot{Q}_{loss} = U_L A_C (T_M - T_a) \quad (6)$$

It's difficult to employ TM when the collector's temperature isn't uniform; this can be remedied by using the heat removal factor (FR). Calculating the heat removal factor $F_R = \frac{\dot{m}C_p(T_{out}-T_{in})}{A_C[I_T(\alpha\tau)-U_L(T_{in}-T_{amb})]}$ (7)

Open Access
Vol. 14, No. 3, September 2024, pp. 135-154
P- ISSN: 2220-5381
E- ISSN: 2710-1096

The useful energy is given by;

$$\dot{Q}_u = F_R A_C [I_T(\alpha\tau) - U_L(T_{in} - T_{amb})] \quad (8)$$

The thermal efficiency of the collector is given by

$$\eta = \frac{\dot{Q}_u}{A_C I_T} = F_R [I_T(\alpha\tau) - U_L(T_{in} - T_{amb})] \quad (9)$$

4.2 Nanofluid properties calculations

The density of the nanofluid is calculated by the followingEquation [22].

$$\rho_{nf} = \rho_{np}(\varphi) + \rho_{bf}(1 - \varphi) \quad (10)$$

The heat capacity of the nanofluid can be evaluated as follows [23].

$$(\rho C_p)_{nf} = (\rho C_p)_{np}(\varphi) + (\rho C_{bf})_{bf}(1 - \varphi) \quad (11)$$

Thermal conductivity of nanofluid is calculated based on the following Equation [22].

$$k_{nf} = k_{bf} \frac{[k_{np} + 2k_{bf} - 2\varphi(k_{bf} - k_{np})]}{[k_{np} + 2k_{bf} + \varphi(k_{bf} - k_{np})]} \quad (12)$$

The viscosity of nanofluid is calculated based on the following Equation [24].

$$\frac{\mu_{nf}}{\mu_{bf}} = \left[\frac{1}{(1-\varphi)^{2.5}}\right] \quad (13)$$

Physical properties of the MWCNT nanoparticles and water at room temperature used in the calculations are presented in Table (2).

Table (2): Physical properties of nanomaterial, water and (MWCNT/DI) nanofluid [25].

Fluid	$\rho(\mathrm{Kg/m^3})$	$\mathrm{C_p(J/Kg.K)}$	$k(\mathrm{W/m.K})$	$\mu(kg.m^{-1}.s^{-1})$
Water	998	4180	0.613	0.0009
MWCNT	2600	730	3000	
(0.01%)MWCNT/ water	998.287	4178.688	0.7696	9.0022×10^{-4}
(0.03%)MWCNT/ water	998.4806	4177.3049	1.08288	9.0067×10^{-4}
(0.05%)MWCNT/ water	998.801	4175.5096	1.39614	9.0112×10^{-4}

Open Access
Vol. 14, No. 3, September 2024, pp. 135-154
P- ISSN: 2220-5381
E- ISSN: 2710-1096

4.3 Overall heat loss coefficient for ETSC

Ref. [26] can be used to derive the overall heat loss coefficient for ETSC, which is separated into losses by the header tube edge and losses by the absorber tube with ambient air:

$$U_L = U_t + U_e \quad (14)$$

$$U_e = \frac{(UA)_P}{A_s} \quad (15)$$

$$U_t = \frac{1}{\frac{1}{h_{ga}} + \frac{1}{h_{pg}}} \quad (16)$$

$$h_{pg} = h_{pgc} + h_{pgd} \text{ [27]} \quad (17)$$

$$h_{pgd} = \frac{\sigma \varepsilon_p}{1 + \frac{\varepsilon_{pd}}{\varepsilon_g d_g}(1 - \varepsilon_p)} \left(T_p^2 + T_g^2\right)\left(T_p + T_g\right) \quad (18)$$

5. Uncertainty Analysis

The error evaluation of the experiment is necessary for faith in the observed results. Uncertainty analysis is used to address the range of uncertainty associated with test results. The general form equation for the uncertainty analysis is provided by:

$$U_y^2 = \sum_{i=1}^{n} U_{xi}^2 \quad (19)$$

Where, U_y is the total uncertainty calculated parameter and Uxi is the uncertainty of each parameter measured.

Input temperature (Tin), exit temperature (Tout), flow rate ($\dot{m}$), and solar intensity (I_T) are the observed parameters of the experiments, with minimal errors in specific heat (CP) and collector area (Ac). As a result, the total uncertainty is as follows:

$$U_y = \eta \times \sqrt{\left(\frac{U_{\dot{m}}}{\dot{m}}\right)^2 + \left(\frac{U_{I_T}}{I_T}\right)^2 + \left(\frac{U_{Tin}}{T_{in}}\right)^2 + \left(\frac{U_{Tout}}{T_{out}}\right)^2} \quad (20)$$

Where, $U_{\dot{m}}$ is the uncertainty for the mass flow rate, measured by flow meter (YF–S201) with uncertainty of 0.05 L/min, $U_{I_T}$is the uncertainty for solar radiation, measured by solar radiation sensor PYR 1307 with uncertainty of 10 W/m^2 while, U_{Tin} and U_{Tout} are the uncertainties for the inlet and outlet temperatures respectively, measured by thermocouples type K with uncertainty of 0.4 ◦C. The total uncertainty for the efficiency of the collector is about 5%.

Open Access
Vol. 14, No. 3, September 2024, pp. 135-154
P- ISSN: 2220-5381
E- ISSN: 2710-1096

Table (3) Shows the uncertainty test for each source.

Parameter	*Uncertainty*
Solar intensity	±1%
Flow rate	±1.5%
Temperature difference	±1.3%

6. Results and Discussion

An investigation into the effect of using deionized water and (MWCNT /DI) as the working fluid with three different flow rates on the temperature difference between the collector's inlet and outlet was carried out in March 2022. The working fluid was pumped through the apparatus at three different flow rates (1,2,3 Lpm) from 9 a.m. to 16 p.m. Every 120 seconds, the temperatures at the inlet, outlet, and throughout the system were recorded. As an average over two-minute intervals, the solar radiation intensity was recorded.

6.1 Temperature Difference Results

The difference in temperature of a fluid between the collector of inlets and outlets is a critical metric for determine the collector performance. Figure (3) illustrates the disparity in temperature between deionized water and nanofluid across various fluid volume flow rates and volume fraction. When employing nanofluids, the temperature differential is greater than when using water. Additionally, the temperature difference increases as the volume fraction of nanoparticles used increases. Furthermore, a smaller mass flow rate produces a greater temperature difference than larger one. For a volume fraction of (MWCNT) nanofluids of (0.05%) compared to water at mass flow rate of (1L/min), the maximum increase in temperature differential are (86.899%). That is caused by the difference in thermal conductivity between nanofluid and water. According to the Table (2), the thermal conductivity of nanofluid is greater for the volume fractions (0.05%) than for (0. 01%).The overall convection heat transfer coefficient increase as thermal conductivity rises. As a result, the fluid's absorption of energy increases and the output temperature rises significantly. As a pump was employed to circulate the fluids, we think that Brownian motion is primarily responsible for the improvement of thermal conductivity of the fluids in our work. the collision between liquid particles and nanoparticles is brought on by the nanoparticles random mobility.

Open Access
Vol. 14, No. 3, September 2024, pp. 135-154
P- ISSN: 2220-5381
E- ISSN: 2710-1096

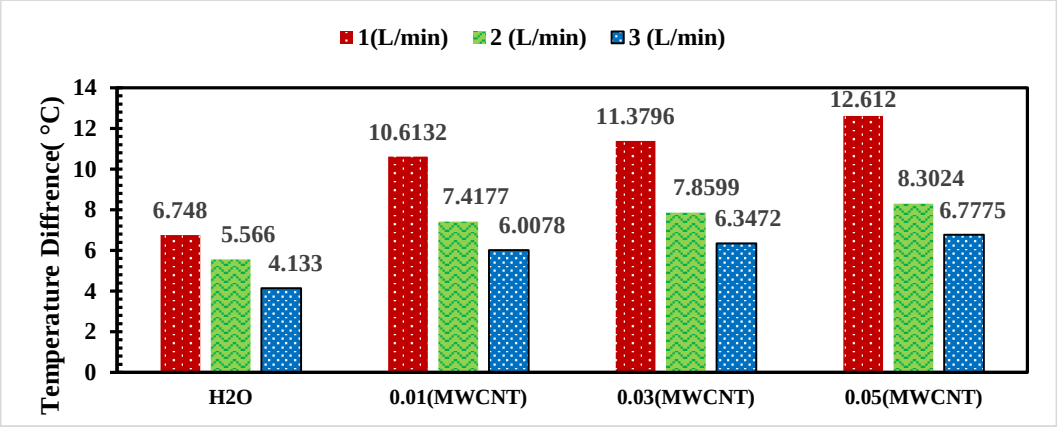

Fig. (3): Temperature difference for deionized water and nanofluids

6.2 Heat Removable Factor Results

factor for heat removal (FR) is an important consideration when testing a solar collector. Eq. (7) can be used to compute it. It is the ratio of the collector's real useable energy gain to the maximum possible heat energy, which can occur if the collector's entire surface temperature is equal to the incoming fluid temperature and heat loss to the surroundings. Simply note that the heat loss calculation is based on the incoming fluid temperature, but there is another temperature at the collector's outlet. The temperature of the output fluid changes when the fluid characteristics change due to the addition of nanoparticles. Figure (4) illustrates various heat removable factor values for water and varied volume fraction nanofluids. The heat removable factor values for water are (0.4407,0.5286 and 0.613) at different values of mass flow rates of (1,2 and 3 L/min), respectively. The values of the heat removable factor when MWCNT nanoparticles with 0.01% volume fraction is added to be (0.5575, 0.687 and 0.797) at the mass flow rates of (1,2and 3 L/min), respectively. when more volume fraction of MWCNT nanoparticles was added to be 0.05% the values of heat removable factor rise to (0.761, 0.7856 and 0.943) at mass flow rates (1,2 and 3 L/min), respectively. The maximum increase in heat removable factor is (53.83%) for the volume fraction 0.05% at mass flow rate (3 L/min) compared with water. For all volume flow rates examined, the heat removable factors for nanofluids are greater than water. Furthermore, when the volume flow rates increases, so do the values of heat removable factors. The explanation is that as the amount of nanoparticles added to the fluid increases, the fluid's exit temperature rises, transferring more heat to the fluid. In the case of increased fluid temperature, however, a lower surface temperature appears, resulting in

Open Access
Vol. 14, No. 3, September 2024, pp. 135-154
P- ISSN: 2220-5381
E- ISSN: 2710-1096

less heat energy loss. As a result, when compared to pure water, nanoparticles increase the actual energy received by the collector.

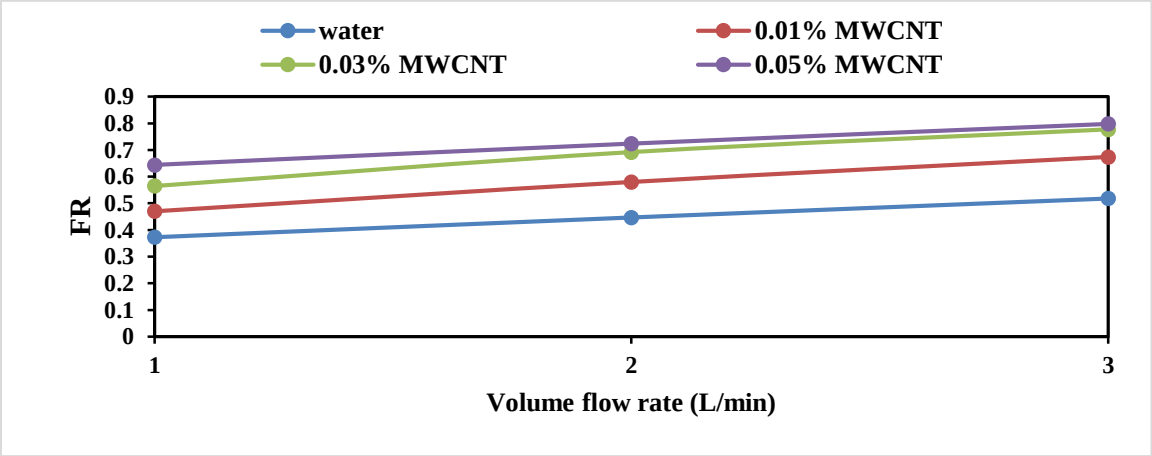

Fig. (4): Heat Removable Factor for deionized water and nanofluids

6.3 Thermal Efficiency Results

In this section, the thermal efficiency of the collector is provided as an independent variable against the lowered temperature parameter, $[(Tin-Tamb)/I_T]$, for all analyzed instances. A linear curve is fitted between thermal efficiency and the lowered temperature parameter, $[(Tin-Tamb)/I_T]$, according to ASHRAE Standard, as Eq. (9). The thermal loss coefficient, $[- F_R UL]$, is the slope of the line. The absorbed energy parameter, $[F_R]$, is the point on the y-axis where the decreased temperature parameter, $[(Tin-Tamb)/I_T]$, equals zero. When $[(Tin-Tamb)/I_T]$ equals zero, the maximum thermal efficiency is obtained, and this thermal efficiency is referred to as the collector's thermo-optical characteristic. An extensive examination of the effect of nanoparticle volume fraction.

6.3.1 Effect of volume fraction of nanoparticles

In this study, we examine three different nanoparticle volume fractions. The minimum and maximum volume fractions used are 0.01% and 0.05%, respectively. In Figures 5(a-c), thermal efficiency is plotted against the decreased temperature parameter, $[(T_{in}-T_{amb})/I_T]$, for both water and nanofluids at varying mass flow rates of (1, 2, and 3) L/min. The explanation of how the solar collector's efficiency changes with the lowered temperature parameter, $[(T_{in}-T_{amb})/I_T]$, is dependent on the value of $[(T_{in}-T_{amb})/I_T]$. The value of the solar collector efficiency at $[(T_{in}-T_{amb})/I_T] = 0$ is known as the collector's thermo-optical characteristic or the absorbed energy parameter, as shown in Figure (6). At volume flow rates of 1, 2, and 3 L/min, the thermo-optical characteristic of the solar

Open Access
Vol. 14, No. 3, September 2024, pp. 135-154
P- ISSN: 2220-5381
E- ISSN: 2710-1096

collector is 0.373, 0.447, and 0.518 for water. As shown in Figure (6), the thermo-optical characteristic of the collector of the solar collector is 0.47, 0.58, and 0.674 for volume flow rates of 1, 2, and 3(L/min) respectively, for the volume fraction of 0.01%. The collector's thermo-optical characteristic for the volume fraction of 0.03% increases from 0.565 for a volume flow rate of 1 (L/min) to 0.692 for a volume flow rate of 2 (L/min) and 0.777 for a volume flow rate of 3 (L/min) and for volume fraction 0.05% the thermo-optical characteristicis 0.644, 0.724 and 0.798 at volume flow rates of (1, 2, and 3) L/min respectively. According to Figures 5(a-c) and 6, the thermo-optical characteristic of the solar collector rises when nanofluids are used instead of water. Adding additional nanoparticles also improves the collector's thermo-optical properties. Furthermore, at larger mass flux rates, the collector's thermo-optical characteristics improve.

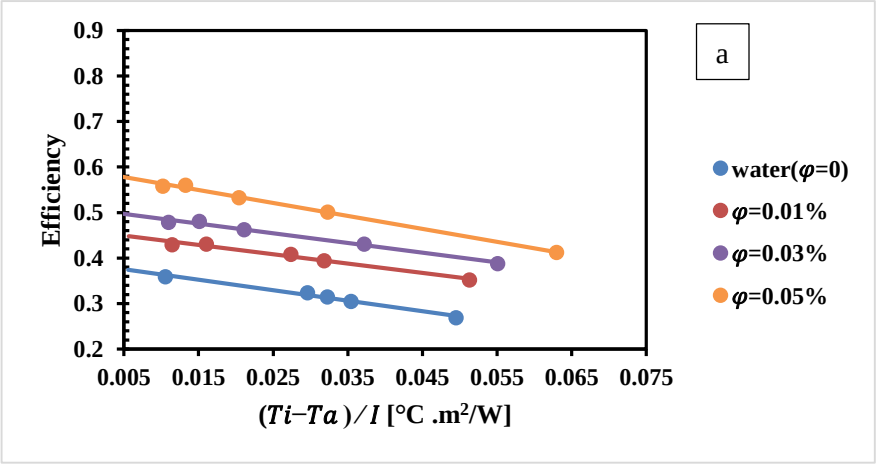

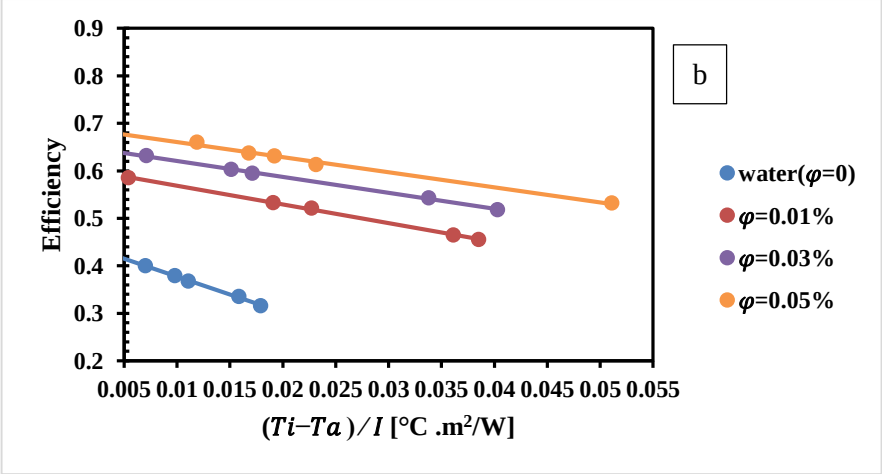

Open Access
Vol. 14, No. 3, September 2024, pp. 135-154
P- ISSN: 2220-5381
E- ISSN: 2710-1096

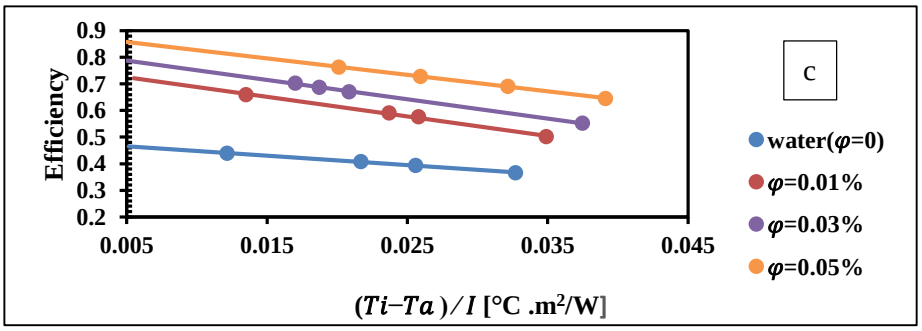

Fig. (5): Linear characteristics for efficiency at different volume flow rate: (a) 1 L/min, (b) 2 L/min, (c) 3 L/min.

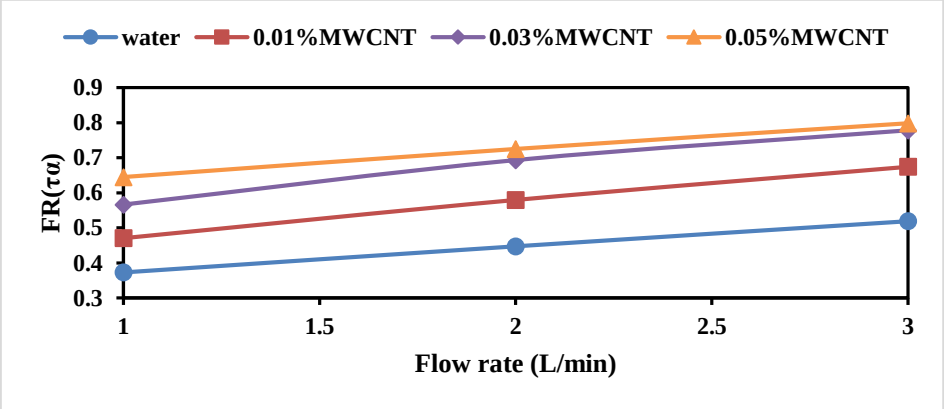

Fig. (6): Absorbed Energy Parameter against volume flow rate for water and nanofluids

6.3.2 Effect of volume flow rate

Figure 7(a-d) shows the effect of the volume flow rate for both water and varying volume fractions of (MWCNT) nanoparticles on the decreased energy parameter, $[(T_{in}-T_{amb})/I_T]$. Figure 7(a) represents water at various volume flow rates. Figure 7(b) shows the volume fraction of 0.01% for volume flow rates of 1, 2, and 3 L/min. Figure **7**(c) depicts the effect of various volume flow rate values of 1, 2, and 3 L/min when a volume fraction of 0.03% MWCNT nanoparticles is utilized. Figure 7(d) depicts the effect of various volume flow rate values of 1, 2, and 3 L/min when a volume fraction of 0.05% MWCNT nanoparticles is utilized. It is obvious that increasing the volume flow rate of the solar collector raises the thermo-optical characteristic of the collector and the thermal loss coefficient. The reason for this is that as the volume flow rate and Reynolds number increase, so does the heat transfer owing to turbulence and mixing between the fluid layers. The reason for this effect is the Brownian motion, which is thought to be the primary cause of nanofluids' higher thermal conductivity when compared to water. The same effect is observed in our studies, implying that higher volume flow rates result in increased

Open Access
Vol. 14, No. 3, September 2024, pp. 135-154
P- ISSN: 2220-5381
E- ISSN: 2710-1096

efficiency in our explored range. Unlike flat plate collectors, evacuated tube collectors have less contact surface between the absorber plate and the moving fluid in the collector's manifold. Due to the reduced contact area, users were obliged to operate the evacuated tube collector at a low pace in order to produce the desired output collector. As a result, this problem provides another impetus for employing nanofluids in evacuated tube solar collectors, as it is discovered that the thermo-optical characteristic of the collector and the thermal loss coefficient are raised when nanofluids are used at the same volume flow as water. We believe that increasing the thermal efficiency of the collector with nanofluids helps to gain more temperature difference, so that when a greater outlet temperature is required, the collector's thermal efficiency must be raised.

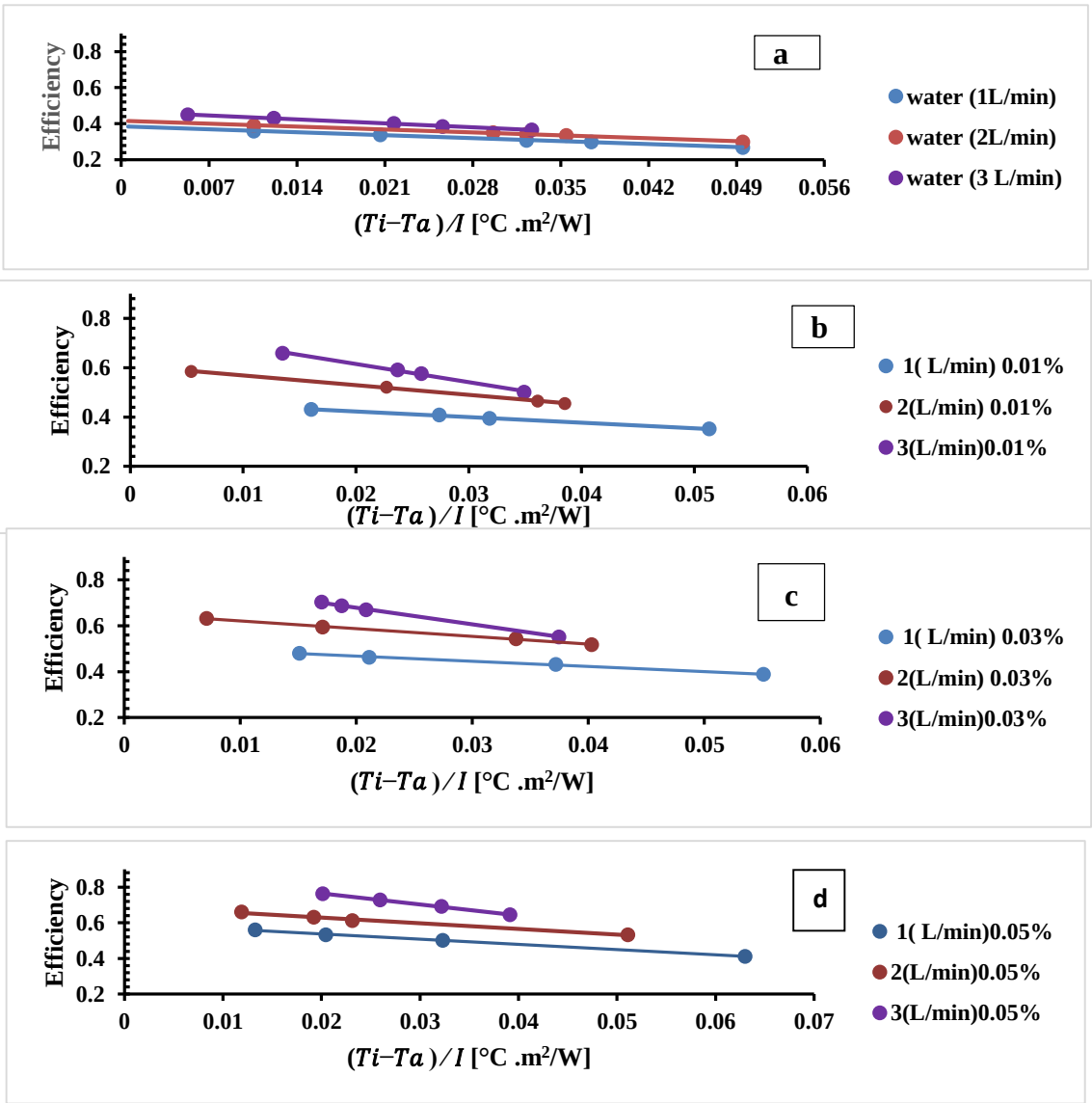

Fig. (7): Linear efficiency characteristics of MWCNT nanoparticles at varying volume fractions: (a) water, (b) 0.01%, (c) 0.03% and (d) 0.05%.

Open Access
Vol. 14, No. 3, September 2024, pp. 135-154
P- ISSN: 2220-5381
E- ISSN: 2710-1096

7. Conclusions:

The influence of (MWCNT) nanoparticles on the performance of the evacuated tube solar collector was investigated experimentally. A comprehensive comparison of water and (MWCNT/water) was carried out. It was created the (MWCNT/water) nanofluid. In the current investigation, various (MWCNT) levels were used. The volume fractions of (MWCNT) nanoparticles were 0.01%, 0.03% and 0.05%, respectively. The trials were carried out at volume flow rates of 1, 2, and 3 (L/min). The performance of the evacuated solar collector was investigated using various variables such as temperature difference and thermal efficiency.

1. The findings show that, employing nanoparticles increases the temperature differential when compared to water.
2. The findings show that as the volume fraction of (MWCNT) nanoparticles increased the temperature difference also increased.
3. When a volume fraction of (MWCNT) nanofluids of 0.05% is used at a volume flow rate of (1L/min), the maximum increase in temperature difference is (86.899%) when compared to water at the same volume flow rate.
4. The thermo-optical characteristic of the evacuated tube solar collector is increased to 86.95% over the entire range investigated.
5. Finally, we can conclude that the majority of our findings clearly show that increasing the volume fraction of (MWCNT) increases the output temperature of the solar collector, enhance the heat transfer to the fluid and the collector's thermo-optical characteristics, but it also increases the thermal loss coefficient.

Nomenclature:

A	Area	(m^2)
C_p	Specific heat capacity	$(J/kg.K)$
d	Outer diameter of the glass	mm
F_R	Heat Removal Factor	
h	Heat transfer coefficient	($W/m^2.K$)
I_T	Total radiation	(W/m^2)
k	Thermal conductivity	$(W/m.K)$
$\dot{m}$	Mass flow rate	(kg/s)
$\dot{Q}$	Heat transfer rate	(W)
T	Temperature	(^oC)
U	Overall heat transfer coefficient	($W/m^2.K$)
$(UA)_P$	Overall heat loss coefficient for the pipe	

Open Access
Vol. 14, No. 3, September 2024, pp. 135-154
P- ISSN: 2220-5381
E- ISSN: 2710-1096

V	Volume	m^3
W	Weight	g

Greek Symbols:

Symbol	Description	Unit
ε	Emissivity	
ρ	Density	(kg/m^3)
α	Collector absorptivity	
η	Thermal efficiency of the collector	
σ	Stefan –Boltzmann constant	$(W/m^2.K^4)$
τ	Glass transmissivity	
φ	Volume fraction of nanoparticles	

Subscript:

Symbol	Description
bf	Base fluid
nf	Nanofluid
np	Nanoparticles
Abs	Absorbed by the collector absorber surface
$loss$	Loss to the ambient
u	Useful gain
c	Collector
s	Outer surface
M	Mean plate
amb	Ambient
g	Outer glass
in	Inlet fluid
out	Outlet fluid
p	Absorber plate
L	Over all
e	Edge of the header tube
t	Between the ambient and absorber tube
ga	The outer glass and environment
pgc	The glass tube and absorber tube
pgd	Across the thermal conductivity

Abbreviation

FPSC	Flat plate solar collector
ETSC	Evacuated tube solar collector
CPVC	Chlorinated Polyvinyl Chloride
UTSC	U tube solar collector

Open Access
Vol. 14, No. 3, September 2024, pp. 135-154
P- ISSN: 2220-5381
E- ISSN: 2710-1096

References:

[1] G. L. Morrison, I. Budihardjo, and M. Behnia, "Water-in-glass evacuated tube solar water heaters", *Sol. Energy*, vol. 76, no. 1–3, pp.135–140, 2004. https://doi.org/10.1016/j.solener.2003.07.024

[2] S. A. Kalogirou, "Solar thermal collectors and applications", *Progress in Energy and Combustion Science*, vol. 30, no. 3, pp. 231–295, 2004. https://doi.org/10.1016/j.pecs.2004.02.001

[3] R. Tang, Y. Yang, and W. Gao, "Comparative studies on thermal performance of water-in-glass evacuated tube solar water heaters with different collector tilt angles", *Solar Energy*, vol. 85, no. 7, pp.1381–1389, 2011. https://doi.org/10.1016/j.solener.2011.03.019

[4] L. M. Ayompe, A. Duffy, M. Mc Keever, M. Conlon, and S. McCormack, "Comparative field performance study of flat plate and heat pipe evacuated tube collectors (ETCs) for domestic water heating systems in a temperate climate", *Energy*, vol. 36, no. 5, pp.3370–3378, 2011. https://doi.org/10.1016/j.energy.2011.03.034

[5] D. Milani, and A. Abbas, "Multiscale modeling and performance analysis of evacuated tube collectors for solar water heaters using diffuse flat reflector", *Renewable Energy*, vol. 86, pp. 360–374, 2016. https://doi.org/10.1016/j.renene.2015.08.013

[6] E. Zambolin, and D. Del Col, "Experimental analysis of thermal performance of flat plate and evacuated tube solar collectors in stationary standard and daily conditions", *Sol. Energy*, vol. 84, no. 8, pp. 1382–1396, 2010. https://doi.org/10.1016/j.solener.2010.04.020

[7] M. A. Sharafeldin, and G. Gróf, "Evacuated tube solar collector performance using CeO_2/water nanofluid", *Journal of Cleaner Production*, vol. 185, pp. 347–356, 2018. https://doi.org/10.1016/j.jclepro.2018.03.054

[8] H. Kim, J. Kim, and H. Cho, "Experimental study on performance improvement of U-tube solar collector depending on nanoparticle size and concentration of Al_2O_3 nanofluid", *Energy*, vol. 118, pp. 1304-1312, 2017. https://doi.org/10.1016/j.energy.2016.11.009

[9] M. A. Sharafeldin, G. Gróf, E. Abu-Nada, and O. Mahian, "Evacuated tube solar collector performance using copper nanofluid: Energy and environmental analysis",

Open Access
Vol. 14, No. 3, September 2024, pp. 135-154
P- ISSN: 2220-5381
E- ISSN: 2710-1096

Applied Thermal Engineering, vol. 162, 114205, 2019. https://doi.org/10.1016/j.applthermaleng.2019.114205

[10] M. Eltaweel, A. A. Abdel-Rehim, and A. A. A. Attia, "Energetic and exergetic analysis of a heat pipe evacuated tube solar collector using MWCNT/water nanofluid", *Case Studies in Thermal Engineering*, vol. 22, 100743, 2021. https://doi.org/10.1016/j.csite.2020.100743

[11] M. R. Abdulwahab, "A numerical investigation of turbulent magnetic nanofluid flow inside square straight channel", *J. Adv. Res. Fluid Mech. Therm. Sci*., vol. 1, no. 1, pp.44–52, 2014.

[12] S. B. Abubakar and N. A. Che Sidik, "Numerical Prediction of Laminar Nanofluid Flow in Rectangular Microchannel Heat Sink", *J. Adv. Res. Fluid Mech. Therm. Sc.*, vol. 7, no. 1, pp. 29–38, Mar. 2015.

[13] N. H. Mohamad Noh, A. Fazeli, and N. A. Che Sidik, "Numerical Simulation of Nanofluids for Cooling Efficiency in Microchannel Heat Sink", *J. Adv. Res. Fluid Mech. Therm. Sc.*, vol. 4, no. 1, pp. 13–23, Dec. 2014.

[14] D. G. Jehad and G. A. Hashim, "Numerical Prediction of Forced Convective Heat Transfer and Friction Factor of Turbulent Nanofluid Flow through Straight Channels", *J. Adv. Res. Fluid Mech. Therm. Sc.*, vol. 8, no. 1, pp. 1–10, Apr. 2015.

[15] S. K. Sharma, and S. M. Gupta, "Preparation and evaluation of stable nanofluids for heat transfer application: a review", *Exp. Therm. Fluid Sci.*, vol. 79, pp. 202–212, 2016. https://doi.org/10.1016/j.expthermflusci.2016.06.029

[16] L. Yang, and K. Du, "A comprehensive review on heat transfer characteristics of TiO_2 anofluids", *Int. J. Heat Mass Transfer*, vol. 108, Part A, pp.11–31, 2017. https://doi.org/10.1016/j.ijheatmasstransfer.2016.11.086

[17] C. S. Nor Azwadi and I. M. Adam, "Turbulent Force Convective Heat Transfer of Hybrid Nano Fluid in a Circular Channel with Constant Heat Flux", *J. Adv. Res. Fluid Mech. Therm. Sc.*, vol. 19, no. 1, pp. 1–9, Mar. 2016.

[18] M. M. Jamil, N. A. Che Sidik, and M. N. A. W. Muhammad Yazid, "Thermal Performance of Thermosyphon Evacuated Tube Solar Collector using TiO2/Water Nanofluid", *J. Adv. Res. Fluid Mech. Therm. Sc.*, vol. 20, no. 1, pp. 12–29, Apr. 2016.

Open Access
Vol. 14, No. 3, September 2024, pp. 135-154
P- ISSN: 2220-5381
E- ISSN: 2710-1096

[19] B. Wei, C. Zou, and X. Li, "Experimental investigation on stability and thermal conductivity of diathermic oil based TiO_2 nanofluids", *Int. J. Heat Mass Transf.*, vol. 104, pp. 537–543, 2017. https://doi.org/10.1016/j.ijheatmasstransfer.2016.08.078

[20] N. A. Che Sidik and A. Safdari, "Modelling of Convective Heat Transfer of Nanofluid in Inversed L-Shaped Cavities", *J. Adv. Res. Fluid Mech. Therm. Sc.*, vol. 21, no. 1, pp. 1–12, May 2016.

[21] S. Kalogirou, "Solar Energy Engineering", vol. 2, Elsevier/ Academic Press., Burlington, MA, 2009.

[22] X. Zhang, H. Gu, and M. Fujii "Effective thermal conductivity and thermal diffusivity of nanofluids containing spherical and cylindrical nanoparticles", Exp. Therm. *Fluid Sci.*, vol.31, pp. 593-599, 2007. https://doi.org/10.1016/j.expthermflusci.2006.06.009

[23] S. Q. Zhou, and R. Ni, "Measurement of the specific heat capacity of water-based Al_2O_3 nanofluid", *Appl. Phys. Lett.*, vol. 92, pp. 1-3, 2008. https://doi.org/10.1063/1.2890431

[24] H. C. Brinkman, "The viscosity of concentrated suspensions and solutions", *The Journal of Chemical Physics*, vol. 20, no. 4, 571, Apr. 1952. https://doi.org/10.1063/1.1700493

[25] J. P. Holman, "Heat transfer, 10th editi. ed.", Mc-GrawHill Higher education, 2010.

[26] Y. Tong, J. Kim, H. Cho, "Effects of thermal performance of enclosed-type evacuated U-tube solar collector with multi-walled carbon nanotube/water nanofluid", *Renew. Energy*, vol. 83, pp. 463–473, 2015. https://doi.org/10.1016/j.renene.2015.04.042

[27] Q. Tian, "Thermal performance of the U-type evacuated glass tubular solar collector", *Build Energy Environ.*, vol. 26, no. 3, pp. 51-54, 2007.